Fluid Phase Equilibria 285 (2009) 36–43

Contents lists available at ScienceDirect

Fluid Phase Equilibria

journal homepage: www.elsevier.com/locate/fluid

Virial coefficients of hard-core attractive Yukawa fluids

D.J. Naresh, Jayant K. Singh*

Department of Chemical Engineering, Indian Institute of Technology Kanpur, Kanpur 208016, India

ARTICLE INFO

Article history:
Received 21 April 2009
Received in revised form 21 June 2009
Accepted 22 June 2009
Available online 28 June 2009

Keywords:
Mayer sampling
Virial coefficient
Yukawa fluid

ABSTRACT

We used Mayer sampling technique—a method based on free energy perturbation, to calculate virial coefficients B_2–B_6 for hard-core Yukawa fluids with interaction range parameter, λ = 1.8, 3.0, 4.0, 5.0, 8.0, 9.0, and 10. We used these coefficients in the virial equation of state (VEOS) to obtain compressibility factor, Z, at super critical temperatures and found to be in excellent agreement with the predictions of equations of state based on mean spherical approximation (EOS-MSA) for Yukawa fluids up to a reduced density, ρ^*, of 0.5. We inspected virial coefficients in representing the PVT behavior along the saturated vapor line of Yukawa fluids. VEOS4, VEOS5 and VEOS6 describe the PVT behavior along the saturated vapor line reasonably good for λ = 1.8, 3.0 and 4.0; and at higher λ, VEOS4 and VEOS5 represent the PVT behavior better than the series that includes B_6. We also report critical properties of Yukawa fluids based on VEOS and compared with the literature values.

1. Introduction

The virial equation of state [1] expresses the deviations from ideal behavior as an infinite power series in ρ:

$$\frac{P}{kT} = \rho + B_2(T)\rho^2 + B_3(T)\rho^3 + B_4(T)\rho^4 + B_5(T)\rho^5 + \cdots\cdots, \quad (1)$$

where P is the pressure, ρ is the number density, k is the Boltzmann constant, T is the absolute temperature, and B_i is the ith virial coefficient. The virial equation of state provides a simple and reliable way to calculate the thermodynamic properties of real gases [2,3]. However, its success depends on the accuracy of the determination of all the virial coefficients up to the given order and convergence of the virial expansion [4]. These coefficients play a vital role in understanding the gas-phase molecular clustering phenomena in simple Lennard-Jones fluids [5] and real fluids such as water [6,7].

Virial coefficients of fluids [8–11] can be determined by a number of different experimental methods [12–14] and from many correlations such as due to Meng et al. [15–18], and Tronopoulos [19,20] which are based on corresponding states principle. These experimental methods and correlations are useful only for the calculation of second and third virial coefficients. In order to calculate higher order integrals, researchers developed molecular based simulation methods such as hit-and-miss Monte Carlo and numerical integration [21,22]. Simple Monte Carlo technique is utilized by Masters and co-workers [23] to evaluate virial coefficients, up to eighth order of, hard convex bodies, hard-spheres with an attractive square-well potential and a two-component mixture of hard-spheres. On the other hand, numerical integration based method is used by Vega and co-workers [21,22,24,25] to calculate second, third and fourth virial coefficients of the two-center Lennard-Jones molecules embedded with point quadrupole and dipole moments.

Recently, Kofke and co-workers introduced Mayer sampling method [26], based on free energy perturbation techniques, for the calculation of higher order virial coefficients. Using this technique, virial coefficients for Lennard-Jones fluid [26], square-well (SW) model potential [27], square-well based model associating fluids [27] and water models [28,29] are determined.

In last few decades many researchers paid much attention to Yukawa model potential since it has ability to represent many real fluid systems ranging from simple [30,31] to complex fluids such as colloidal suspensions [30,32,33], proteins [34,35], polymer solutions [36], ionic fluids [37], molten salts and liquid metals [38,39], alloys [40] and dilute solutions of strong electrolytes [41]. An attractive element of one-Yukawa potential and multi-Yukawa [33,42,43] model potential is that analytical solution of the Ornstein-Zernike integral equation is feasible within the mean spherical approximation (MSA) [44–47] approach. Using these explicit analytical solutions based on MSA numerous researchers predicted the structure, thermodynamic properties [46–49] and phase equilibria [47,48,50] of pure and binary mixtures of hard-core Yukawa fluids of variable range.

The Yukawa potential [41] is given by the following expression:

$$u(r) = \begin{cases} \infty, r \le \sigma \\ -\varepsilon \dfrac{\exp[-\lambda(r/\sigma - 1)]}{r/\sigma}, r \ge \sigma \end{cases}, \quad (2)$$

* Corresponding author.
E-mail address: jayantks@iitk.ac.in (J.K. Singh).

0378-3812/$ – see front matter © 2009 Elsevier B.V. All rights reserved.
doi:10.1016/j.fluid.2009.06.019

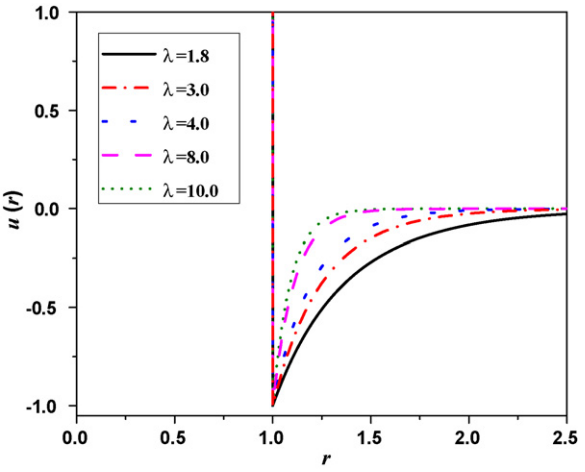

Fig. 1. Hard-core Yukawa potential with various interaction ranges.

where ε is the potential depth, σ is the molecular diameter and λ is the range of interaction. The limit $\lambda \to \infty$ corresponds to a hard-sphere potential. The Yukawa potential with various values of λ is shown in Fig. 1.

In recent years molecular simulation has become a successful tool in estimating the properties of bulk Yukawa fluids [48,51,52] and their mixtures [53,54]. Such calculations are being conducted using canonical ensemble Monte Carlo (CMC) [48,55] and canonical ensemble molecular dynamics (CMD) [55] for structure and thermodynamic properties. However, for phase equilibria calculations Gibbs ensemble Monte Carlo (GEMC) [48,56,57] and grand-canonical transition matrix Monte Carlo (GC-TMMC) [51] techniques have been used preferentially.

In the present work, we apply Mayer sampling technique to find virial coefficients for hard-core Yukawa fluids with interaction range, λ, ranging from 1.8 to 10 and consequently various different analysis has been done using viral equation of state. In this work, we adopt units such that ε and σ are unity. Reduced units used in this study are: temperature $T^* = kT/\varepsilon$, density $\rho^* = \rho\sigma^3$, pressure $P^* = P\sigma^3/\varepsilon$ and virial coefficients $B_i{}^* = B_i/b^{i-1}$, where B_i is the ith virial coefficient and $b = 2\pi\sigma^3/3$ is the second virial coefficient of the hard-sphere. The rest of the paper proceeds as follows: In the next section, we briefly outline the Mayer sampling methodology together with MSA EOS; the results and discussions are given in sec III and finally, concluding remarks in sec IV.

2. Methodology

In this work, we use Mayer sampling method, to evaluate virial coefficients. Complete description of the method is given elsewhere [6,26–29]. However, we briefly illustrate the methodology here. The method is based on performing molecular simulation on the molecules represented in the cluster integral appearing in the statistical mechanical formulation of virial coefficients. In this method, first, we generate configurations of molecules using Metropolis MC [58] with importance sampling based on the magnitude of the interactions represented in the cluster integral. Second, we need to evaluate the ratio of the desired cluster integral to a known reference integral. We do not attempt to evaluate the cluster integral directly. The umbrella sampling method provides one such formula

$$\Gamma(T) = \Gamma_0 \frac{\Gamma}{\Gamma_0} = \Gamma_0 \frac{\langle \gamma/\pi \rangle_\pi}{\langle \gamma_0/\pi \rangle_\pi}. \tag{3}$$

In the above expression, $\Gamma(T)$ represents a cluster integral or sum of integrals with integrand γ (r^n; T). The angle brackets indicate the "ensemble average" integral over all configurations and orientations of the n molecules, and the subscript π indicates that the integral is weighted by the normalized π distribution. The subscript '0' indicates a quantity for a reference system, for which Γ_0 is known. The method involves perturbations directly between the target system (which governs sampling) and the reference system.

There are many choices one can select for the π distribution and the reference cluster [26]. In this work we have used $\pi = |\gamma\ (r^n; T)|$, as suggested by the importance sampling approach. We use π as the absolute value of the sum of all clusters. By choosing this definition for π, the Eq. (3) can be expressed as

$$\Gamma(T) = \Gamma_0 \frac{\langle sgn(\gamma) \rangle_\pi}{\langle \gamma_0/\pi \rangle_\pi}, \tag{4}$$

where sgn (γ) is just the sign of the cluster sum. Therefore, each term in numerator average is +1 or −1.

Regarding the reference cluster one must select a system whose phase space is a subset of the phase space of the target system [59,60]. In this work, we use the ring-shaped cluster with a hard-sphere potential as a reference for sampling simulations.

The virial coefficient calculations of Yukawa fluids are conducted as follows. MC sampling is performed for a number of molecules equal to the order of the virial coefficient being computed. Trial configurations are generated using molecular displacement MC move and cluster MC moves [26] for Yukawa fluids. Each trial is accepted with probability min (1, π^{new}/π^{old}), where π is defined as the absolute value of the weighted sum of the cluster integrands contributing to the calculated virial coefficient. The value of a cluster for a given configuration is determined by summing the contributions of all unique permutations of the labeling of the molecules. In this work, 10^9 configurations are generated for the estimation of virial coefficients. Step sizes for the trials were adjusted in a short "equilibration" period, before accumulating averages, to achieve a 50% acceptance rate for trial moves.

Virial coefficients up to B_4 can easily be calculated within 24 h on a single core of quad core processor. For higher-order coefficients (B_5 and B_6), longer runs are required to collect the required number of configurations. For example, calculating B_5 at a given temperature required 95–100 h on a single core of quad core Intel 2.66 GHz processor to generate 10^9 configurations. In this work, four independent runs are conducted to obtain the statistical error. All simulations in this work are performed with the etomica molecular simulation suite [61].

One of the main objectives of this work is to compare the VEOS with the literature data available. We have taken molecular simulation data wherever available however analytical expression based on MSA is also solved for the comparison. The following describe briefly the MSA theory.

Explicit analytical expressions for the Helmholtz free energy, A, can be expressed in terms of the inverse temperature expansion of the MSA free energy [44,48]:

$$\begin{aligned} \frac{A}{NkT} &= \frac{A_0}{NkT} + \sum_{n=1}^{5} \frac{A_n}{NkT} \\ \frac{A_0}{NkT} &= \frac{A^{HS,ex}}{NkT} + \frac{A^{id}}{NkT}, \\ \frac{A^{id}}{NkT} &= \ln \rho^* - 1 \end{aligned} \tag{5}$$

where, $\rho^* = \rho\sigma^3$ is the reduced density, A_0 and A^{id} is the Helmoltz free energy of the hard-sphere and the ideal gas, respectively. The above expression of A^{id} corresponds to sigma as the de Broglie wave length. The excess free energy of a hard-sphere fluid, $A^{HS,ex}$ is given by Carnahan and Starling [62] expression:

$$\frac{A^{HS,ex}}{NkT} = \eta \frac{(4 - 3\eta)}{(1 - \eta)^2}, \tag{6}$$

where, $\eta = \pi\rho\sigma^3/6$ is the packing density. The expression for the free energy in Eq. (5) is given by Henderson et al. [63].

$$\frac{A_n}{NkT} = -\frac{v_n}{2n}\left(\frac{\varepsilon}{kT}\right)^n + F_n\left(\frac{\varepsilon}{kT}\right)^n, \tag{7}$$

where

$$\begin{aligned}
v_1 &= 2\alpha_0/\phi_0,\\
v_2 &= -2w(\alpha_1 - 1 - \alpha_0\psi)/(\lambda\phi_0),\\
v_3 &= -2w^2(\alpha_1 - 1 - \alpha_0\psi)(1 + 3\lambda\psi)/(\lambda^3\phi_0),\\
v_4 &= -4w^3(\alpha_1 - 1 - \alpha_0\psi)(1 + 4\lambda\psi + 6\lambda^2\psi^2)/(\lambda^5\phi_0),\\
v_5 &= -10w^4(\alpha_1 - 1 - \alpha_0\psi)(1 + 5\lambda\psi + 11\lambda^2\psi^2 + 11\lambda^3\psi^3)/(\lambda^7\phi_0),
\end{aligned} \tag{8}$$

$$\begin{aligned}
\alpha_0 &= L(\lambda)/(\lambda^2(1-\eta)^2),\\
\alpha_1 &= 12\eta(1 + \lambda/2)/(\lambda^2(1-\eta)),\\
\phi_0 &= (\exp(-\lambda)L(\lambda) + S(\lambda))/(\lambda^3(1-\eta)^2),\\
\psi &= \lambda^2(1-\eta)^2\frac{(1-\exp(-\lambda))}{(\exp(-\lambda)L(\lambda) + S(\lambda))} - 12\eta(1-\eta)\frac{(1-\lambda/2) - (1+\lambda/2)\exp(-\lambda)}{(\exp(-\lambda)L(\lambda) + S(\lambda))},
\end{aligned} \tag{9}$$

$$\begin{aligned}
w &= 6\eta/\phi_0^2,\\
L(\lambda) &= 12\eta((1 + \eta/2)\lambda + 1 + 2\eta),\\
S(\lambda) &= (1-\eta)^2\lambda^3 + 6\eta(1-\eta)\lambda^2 + 18\eta^2\lambda - 12\eta(1 + 2\eta),
\end{aligned} \tag{10}$$

$$\begin{aligned}
F_1 &= F_2 = 0,\\
F_3 &= -\frac{2\eta((1-\eta)^4)^2}{((1+2\eta)^2)^2(1+3\lambda)},\\
F_4 &= -\frac{\eta((1-\eta)^4)^3}{((1+2\eta)^2)^3(4(1+2\lambda))},\\
F_5 &= -\frac{\eta((1-\eta)^4)^4}{((1+2\eta)^2)^4(10(3+5\lambda))}.
\end{aligned} \tag{11}$$

Note that F_n terms are based on the compressibility approximation [64]. The corresponding analytical expressions for the compressibility factor ($Z = PV/NkT$) and internal energy (U/NkT) can be obtained as follows:

$$\begin{aligned}
Z &= \sum_{n=1}^{5} Z_n = \sum_{n=1}^{5}\frac{P_n V}{NkT},\\
Z_n &= \frac{\eta\partial(A_n/NkT)}{\partial\eta},\\
\frac{U}{NkT} &= \sum_{n=1}^{5}\frac{U_n}{NkT},\\
\frac{U_n}{NkT} &= \frac{-T^*\partial(A_n/NkT)}{\partial T^*}.
\end{aligned} \tag{12}$$

where, $T^* = kT/\varepsilon$.

The excess chemical potential can be given by

$$\frac{\mu^{ex}}{kT} = \frac{A^{ex}}{NkT} + \frac{PV}{NkT} - 1. \tag{13}$$

In order to account the higher order terms, we used the Pade's approximation,

$$\frac{A^{Pade}}{NkT} = \frac{A_0}{NkT} + \frac{A_1}{NkT} + \frac{A_2}{NkT} + \frac{A_3}{NkT} + \frac{A_4}{NkT}\left(1 - \frac{A_5/NkT}{A_4/NkT}\right)^{-1}, \tag{14}$$

Table 1
Virial coefficients of a Yukawa fluid with interaction range, $\lambda = 1.8$, as calculated using Mayer sampling method. Numbers in the subscript indicate the 67% confidence limits of the last digit of the reported value.

T^*	B_2/b	B_3/b^2	B_4/b^3	B_5/b^4	B_6/b^5
0.7	-3.859_2	-1.1689_{19}	-11.738_{18}	-102.26_{15}	-859_{48}
0.8	-3.088_1	-0.1184_2	-2.939_3	-19.01_{40}	-126_{12}
0.9	-2.5287_3	0.2791_2	-0.593_3	-3.736_{20}	-17.07_{97}
1.0	-2.1043_5	0.4336_{10}	0.0624_{32}	-0.607_{11}	-2.419_{156}
1.15	-1.6303_3	0.4998_2	0.2474_{12}	0.0442_{18}	-0.107_{41}
1.5	-0.9395_3	0.4815_1	0.1867_3	0.0063_{19}	-0.027_{20}
2.0	-0.4108_1	0.4433_1	0.1573_1	0.0449_5	0.0465_{76}
3.0	0.0870_1	0.4370_1	0.1994_3	0.1106_1	0.0664_{10}
5.0	0.4646_1	0.4754_1	0.2520_1	0.1260_1	0.0479_4
10.0	0.7371_1	0.5354_1	0.2810_1	0.1191_1	0.0393_1
20.0	0.8697_1	0.5764_1	0.2875_1	0.1140_1	0.0382_1

Table 2
Virial coefficients of a Yukawa fluid with interaction range, $\lambda = 3.0$, as calculated using Mayer sampling method. Numbers in the subscript indicate the 67% confidence limits of the last digit of the reported value.

T^*	B_2/b	B_3/b^2	B_4/b^3	B_5/b^4	B_6/b^5
0.6	-2.2425_3	0.2832_6	-0.2822_{60}	-2.136_{16}	-11_2
0.65	-1.8920_2	0.4479_7	0.2317_{43}	-0.100_{13}	-0.45_{31}
0.7	-1.6091_4	0.5064_4	0.3266_{64}	0.114_{14}	-0.230_{63}
0.75	-1.3771_2	0.5168_2	0.2916_{24}	0.0539_{76}	-0.728_{102}
1.0	-0.6445_1	0.4321_1	0.1119_4	-0.0451_{21}	-0.0049_{60}
1.2	-0.3188_1	0.3855_1	0.0987_3	0.0185_3	0.0547_{40}
1.5	-0.0169_1	0.3629_1	0.1278_1	0.0726_6	0.0584_{25}
2.0	0.2639_1	0.3735_1	0.1759_1	0.1011_2	0.0499_8
3.0	0.5258_1	0.4207_1	0.2245_1	0.1118_1	0.0449_2
5.0	0.7223_1	0.4853_1	0.2564_1	0.1136_2	0.0417_1
10.0	0.8641_1	0.5489_1	0.2743_1	0.1128_1	0.0397_1
20.0	0.9327_1	0.5854_1	0.2812_1	0.1118_1	0.0389_1

$$Z^{pade} = Z^{HS} + Z_1 + Z_2 + Z_3 + Z_4\left(1 - \frac{A_5/NkT}{A_4/NkT}\right) + \frac{A_4}{NkT}\left(\frac{Z_5}{A_4/NkT} - \frac{Z_4A_5/NkT}{(A_4/NkT)^2}\right), \tag{15}$$

$$\frac{U^{pade}}{NkT} = \frac{U_1}{NkT} + \frac{U_2}{NkT} + \frac{U_3}{NkT} + \frac{U_4}{NkT}\left(1 - \frac{A_5/NkT}{A_4/NkT}\right) + \frac{A_4}{NkT}\left(\frac{U_5/NkT}{A_4/NkT} - \frac{(U_4/NkT)(A_5/NkT)}{(A_4/NkT)^2}\right). \tag{16}$$

The compressibility factor of the hard-sphere fluid is obtained from the following expression, given by Carnahan and Starling [62]:

$$Z^{HS} = \frac{(1 + \eta + \eta^2 - \eta^3)}{(1-\eta)^3}. \tag{17}$$

In this work, we used Eq. (15) to calculate compressibility factor (Z) based on EOS-MSA for comparison with that due to virial equation of state (VEOS).

3. Results and discussion

We start our discussion on the behavior of B_2^*–B_6^* of hard-core Yukawa fluids as a function of temperature and interaction range. Tables 1–7 present virial coefficients of hard-core Yukawa fluids, up to sixth order, at various interaction range, $\lambda = 1.8$, 3.0, 4.0, 5.0, 8.0, 9.0, and 10.0, due to Mayer sampling. Figs. 2 and 3 present a plot of B_3^* and B_4^*, respectively, as a function of temperature for Yukawa fluids of different interaction ranges. B_3^* is observed to be negative at sub critical temperature, as seen also for LJ [26], SW and

Table 3
Virial coefficients of a Yukawa fluid with interaction range, λ = 4.0, as calculated using Mayer sampling method. Numbers in the subscript indicate the 67% confidence limits of the last digit of the reported value.

T^*	B_2/b	B_3/b^2	B_4/b^3	B_5/b^4	B_6/b^5
0.5	-2.0931_1	0.3153_{22}	0.0113_{57}	-0.905_{73}	-4.4_9
0.53	-1.8191_3	0.4483_7	0.3314_{39}	0.102_{16}	0.330_{54}
0.56	-1.5891_4	0.5042_5	0.3807_{63}	0.188_7	-1.32_{17}
0.7	-0.8718_1	0.4620_3	0.1429_{11}	-0.098_2	-0.063_{69}
1.0	-0.1718_1	0.3355_2	0.0795_2	0.0344_7	0.0488_{77}
1.2	0.0623_1	0.3209_1	0.1121_1	0.0684_3	0.0469_{10}
1.5	0.2786_1	0.3324_2	0.1527_3	0.0871_1	0.0420_4
2.0	0.4790_1	0.3705_1	0.1927_1	0.0977_3	0.0415_1
3.0	0.6651_1	0.4336_1	0.2284_1	0.1046_1	0.0411_1
5.0	0.8046_1	0.5004_1	0.2534_1	0.1085_1	0.0402_2
10.0	0.9043_1	0.5592_1	0.2706_1	0.1102_1	0.0394_1
20.0	0.9526_1	0.5913_1	0.2787_1	0.1103_1	0.0390_1

Table 4
Virial coefficients of a Yukawa fluid with interaction range, λ = 5.0, as calculated using Mayer sampling method. Numbers in the subscript indicate the 67% confidence limits of the last digit of the reported value.

T^*	B_2/b	B_3/b^2	B_4/b^3	B_5/b^4	B_6/b^5
0.45	-1.8931_5	0.3892_4	0.3003_{85}	0.125_{72}	0.976_{63}
0.51	-1.3439_1	0.5118_2	0.3417_{22}	0.039_{18}	-0.521_{104}
0.6	-0.8204_2	0.4424_1	0.1193_2	-0.107_4	-0.071_{83}
0.7	-0.4564_2	0.3604_1	0.0526_4	-0.0343_9	0.029_8
1.0	0.0919_2	0.2904_1	0.0991_1	0.0611_2	0.0350_{10}
1.2	0.2744_1	0.3011_1	0.1339_2	0.0755_3	0.0359_8
1.5	0.4428_1	0.3327_2	0.1678_1	0.0851_1	0.0368_2
2.0	0.5982_1	0.3832_1	0.1992_2	0.0932_1	0.0378_4
3.0	0.7421_1	0.4503_1	0.2286_1	0.1005_1	0.0390_1
5.0	0.8497_1	0.5144_1	0.2515_1	0.1054_1	0.0391_1
10.0	0.9264_1	0.5677_1	0.2689_1	0.1083_1	0.0389_1
20.0	0.9636_1	0.5958_1	0.2778_1	0.1094_1	0.0387_1

Table 5
Virial coefficients of a Yukawa fluid with interaction range, λ = 8.0, as calculated using Mayer sampling method. Numbers in the subscript indicate the 67% confidence limits of the last digit of the reported value.

T^*	B_2/b	B_3/b^2	B_4/b^3	B_5/b^4	B_6/b^5
0.35	-1.3968_1	0.3170_{13}	0.2798_{170}	0.210_{79}	-9_2
0.4	-1.1823_2	0.4722_6	0.2702_{53}	-0.0453_{119}	-1.13_{86}
0.5	-0.4632_1	0.3227_1	0.0291_6	-0.0403_{18}	0.057_{35}
0.6	-0.0942_2	0.2493_1	0.0434_1	0.0273_8	0.0237_{70}
0.7	0.1280_1	0.2364_1	0.0776_1	0.0463_3	0.0241_{10}
1.0	0.4599_1	0.2878_1	0.1394_1	0.0657_1	0.0279_3
1.5	0.6703_1	0.3771_3	0.1839_1	0.0804_1	0.0320_2
2.0	0.7628_2	0.4326_2	0.2068_1	0.0879_1	0.0340_1
3.0	0.8481_1	0.4933_1	0.2313_1	0.0953_1	0.0358_1
5.0	0.9116_1	0.5446_1	0.2523_1	0.1013_1	0.0371_1

Table 6
Virial coefficients of a Yukawa fluid with interaction range, λ = 9.0, as calculated using Mayer sampling method. Numbers in the subscript indicate the 67% confidence limits of the last digit of the reported value.

T^*	B_2/b	B_3/b^2	B_4/b^3	B_5/b^4	B_6/b^5
0.34	-1.7016_5	0.3801_{19}	0.3675_{143}	0.258_{69}	-5_2
0.35	-1.5357_2	0.4361_{21}	0.4029_{63}	0.179_{35}	-3_2
0.4	-0.9307_2	0.4279_8	0.1470_{46}	-0.1220_{80}	-0.653_{172}
0.5	-0.2923_1	0.2734_3	0.0222_2	-0.0047_4	0.0133_{47}
0.6	0.0346_1	0.1703_1	0.0571_2	0.0366_3	0.0210_{64}
0.7	0.2311_1	0.2312_4	0.0904_1	0.0487_2	0.0225_{10}
1.0	0.5245_1	0.3007_1	0.1456_1	0.0656_1	0.0274_3
1.5	0.7100_2	0.3928_1	0.1870_1	0.0800_1	0.0313_2
2.0	0.7915_1	0.4467_1	0.2092_1	0.0873_1	0.0334_2
3.0	0.8665_1	0.5040_1	0.2330_1	0.0948_1	0.0353_1
5.0	0.9224_1	0.5516_1	0.2536_1	0.1009_1	0.0368_1

Table 7
Virial coefficients of a Yukawa fluid with interaction range, λ = 10.0, as calculated using Mayer sampling method. Numbers in the subscript indicate the 67% confidence limits of the last digit of the reported value.

T^*	B_2/b	B_3/b^2	B_4/b^3	B_5/b^4	B_6/b^5
0.33	-1.5943_8	0.4051_{40}	0.3945_{121}	0.308_{30}	5.73_{84}
0.34	-1.4250_3	0.4443_{19}	0.3562_{179}	0.156_{81}	6.26_{47}
0.4	-0.7313_2	0.3753_3	0.0694_{19}	-0.1013_{86}	0.08_{18}
0.5	-0.1572_2	0.2396_1	0.0289_3	0.0163_7	0.015_{44}
0.6	0.1362_1	0.2166_1	0.0699_1	0.0404_2	0.0192_{32}
0.7	0.3126_2	0.2335_1	0.1004_1	0.0497_1	0.0216_2
1.0	0.5753_1	0.3149_1	0.1506_1	0.0660_1	0.0268_3
1.5	0.7412_1	0.4073_1	0.1902_1	0.0799_1	0.0309_1
2.0	0.8140_1	0.4592_1	0.2118_1	0.0868_5	0.0330_1
3.0	0.8810_1	0.5133_1	0.2350_1	0.0946_2	0.0349_1
5.0	0.9308_1	0.5576_1	0.2549_1	0.1006_2	0.0364_1

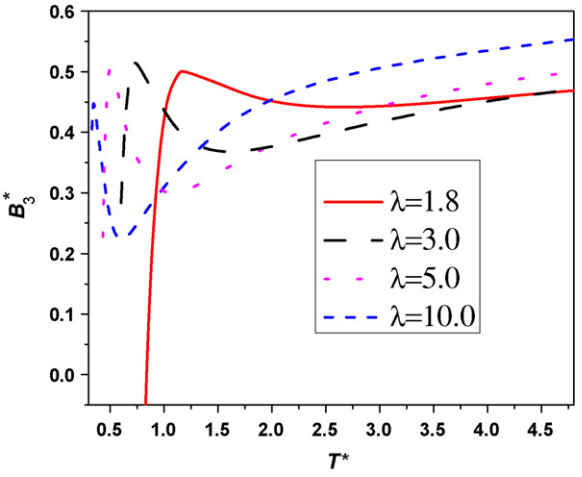

Fig. 2. Temperature dependence of B_3^* of Yukawa fluids at λ = 1.8, 3.0, 4.0, 5.0, 8.0. 9.0 and 10.0.

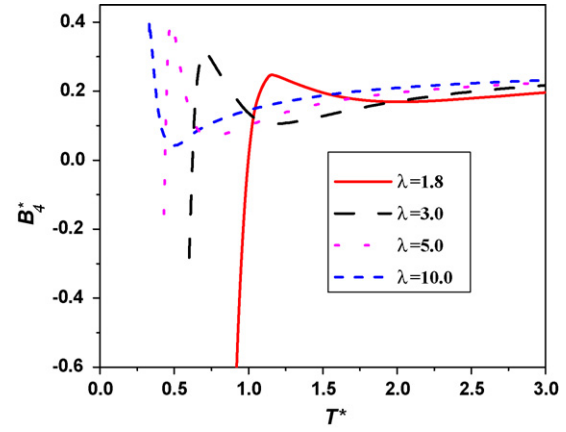

Fig. 3. Temperature dependence of B_4^* of Yukawa fluids at λ = 1.8, 3.0, 4.0, 5.0, 8.0. 9.0 and 10.0.

associating fluids [27], and quadrupolar two center LJ fluids [24], and it increases sharply and becomes positive and goes through a maxima. The peak at which B_3^* is maximum occurs at lower temperature as λ increases. Subsequent increase in temperatures decays B_3^* slowly to a minima. The temperature at which the minima occurs decreases with increasing λ. Further, increase in the temperature, gradually increases the third virial coefficient of Yukawa fluid; with rate of increase increases with the decreases in the attractive range of the fluid. The observed trends for B_4^* are qualitatively similar to those observed for B_3^*. However, at a substantial high temper-

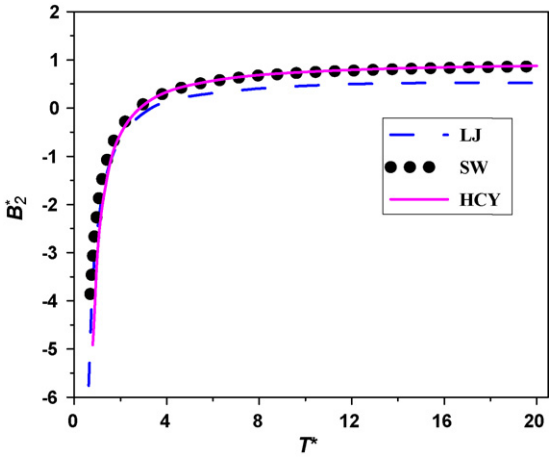

Fig. 4. Comparison plot of B_2^* for square-well fluid with well-extent 1.5, Lennard-Jones fluid and Yukawa fluid at $\lambda = 1.8$.

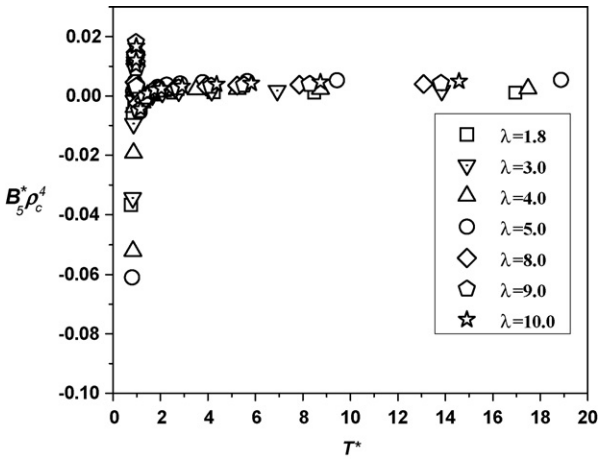

Fig. 6. Corresponding plot of B_5^* for Yukawa fluids at various interaction ranges.

ature (beyond the range presented in the plot), B_3^* of all Yukawa fluids with various interaction ranges appears to approach a common value. It is interesting to observe that this common value is very close to the third virial coefficient of the hard-sphere potential model. This behavior is found for all the virial coefficients. For example, at $\lambda = 1.8$ and $T^* = 20$, B_3^* and B_4^* are =0.5764 and 0.2875, respectively. These values are very close to that of hard-sphere particles, for which $B_3^* = 0.625$ and $B_4^* = 0.2869$.

Figs. 4 and 5 present the comparison of virial coefficients of Lennard-Jones, square-well (SW) fluid with well-extent, 1.5 and Yukawa fluid with interaction range parameter, $\lambda = 1.8$ for B_2^* and B_6^*, respectively. At lower temperature range, B_2^* for all the three fluids falls on a master curve, but at higher temperature range B_2^* values of Lennard-Jones fluid are slightly less compared to SW and Yukawa fluids. On the other hand, the trends are quite distinct for B_6^*, as shown in Fig. 5, where B_6^* values are different for all the three potential forms over the entire temperature range; though the qualitative behavior is same. This suggests the nature of the potential (soft or hard) apparently affects significantly the large cluster behavior as opposed to that of smaller cluster.

In our earlier study on SW fluids [27], we observed a corresponding state plot of virial coefficient for variable interaction range. Similar investigation is performed in this work. It is interesting to observe that all the calculated virial coefficients for Yukawa fluids fall (approximately) on one master curve in a corresponding state plot, $B_i^* \rho_c^{*i}$ vs. T/T_c, where B_i^*, T_c^* and ρ_c^* (taken from [51]), are the ith virial coefficient, critical temperature and critical density, respectively. Fig. 6 presents a typical corresponding state plot of B_5^*, where it is noted that data are not exactly on a master curve at higher temperatures, which may be due to the error associated with the critical properties.

Having determined virial coefficients B_2^*–B_6^* for Yukawa fluids, we now turn our attention to calculate thermodynamic properties using virial equation of state. Before proceeding for these calculations, we investigated the range of applicability of VEOS. Fig. 7 shows the plots of Z vs. density, ρ^*, predicted by the sixth order (VEOS6) virial EOS and compared with the predictions of EOS based on MSA (EOS-MSA) for Yukawa fluids at $\lambda = 1.8$. VEOS6 provides excellent agreement up to a reduced density of 0.5 at super critical temperatures ($T^* = 1.5$ and 2.0); while at sub-critical temperature ($T^* = 1.0$), VEOS6 begins to fail at about ρ^* of 0.23. Similar observations are also found at other interaction ranges (figures are not shown).

We examined the ability of different truncated virial EOS to predict the PVT behavior along the saturated vapor line of Yukawa fluids. We compared the predictions of second, third, fourth, fifth and sixth order truncated virial EOS with molecular simulation data [51] available in the literature. Figs. 8 and 9 present a typical plots

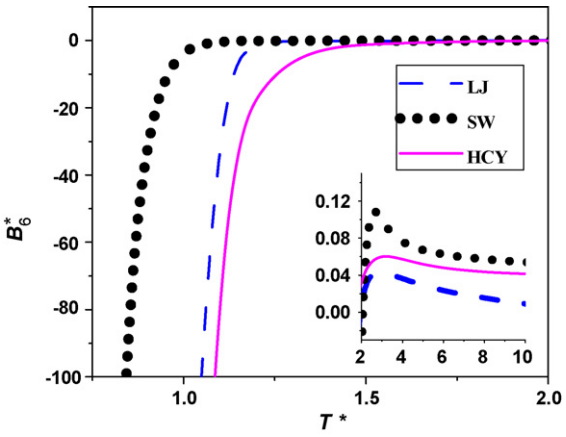

Fig. 5. Comparison plot of B_6^* for square-well fluid with well-extent 1.5, Lennard-Jones fluid and Yukawa fluid at $\lambda = 1.8$. Inset compares the B_6^* data for all three fluids at higher temperatures.

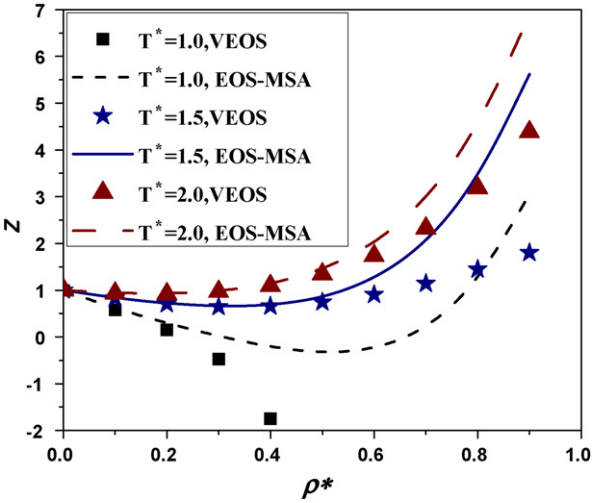

Fig. 7. Compressibility factor of hard-core Yukawa fluid with interaction range, $\lambda = 1.8$. Curves represent the data based on the sixth order (VEOS6) virial EOS and symbols denote EOS-MSA results.

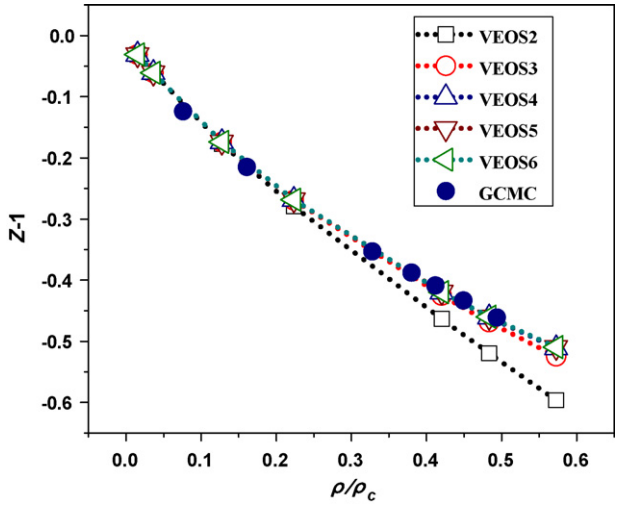

Fig. 8. Deviation from ideality along the saturated vapor line of hard-core Yukawa fluid at λ = 1.8. Filled symbol correspond to the data due to GC-TMMC simulations [51] and open symbols correspond to different truncated virial EOS. Lines are provided to guide the eye.

of deviation from ideality, $Z-1$, against reduced density, ρ_r^*, predicted by the different truncated virial series and from molecular simulation data along the saturated vapor line of Yukawa fluids at interaction range parameter, λ = 1.8 and 10.0, respectively. Fig. 8 shows that second order (VEOS2) virial series predictions of non-ideality are in good accordance with the literature data up to a reduced density of 0.15. With the addition of third virial coefficient, range of applicability of VEOS increases up to the reduced density of 0.42. VEOS4 based prediction is reasonably good until reduced density of 0.57. The behavior of VEOS is not affected by the presence of 5th and 6th virial coefficients. For the present density range available in the literature, deviation from ideality (Z – 1) based on VEOS4, VEOS5 and VEOS6 fall within 1% of the literature data. Similar observations are found at other interaction ranges, λ = 3.0 and 4.0. However, at higher interaction ranges, λ = 8.0, 9.0 and 10.0 VEOS4 and VEOS5 predictions are found to be in good agreement with literature data as shown in Fig. 9 for the interaction range 10.0. In this case VEOS6 fails at higher densities. In summary, at any given interaction range,λ, and density VEOS4 is the most use-

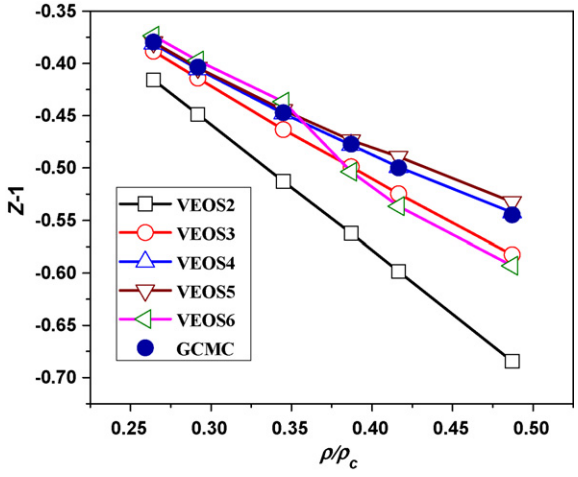

Fig. 9. Deviation from ideality along the saturated vapor line of hard-core Yukawa fluid at λ = 10.0. Filled symbol correspond to data due to GC-TMMC simulations [51] and open symbols correspond to different truncated virial EOS. Lines are provided to guide the eye.

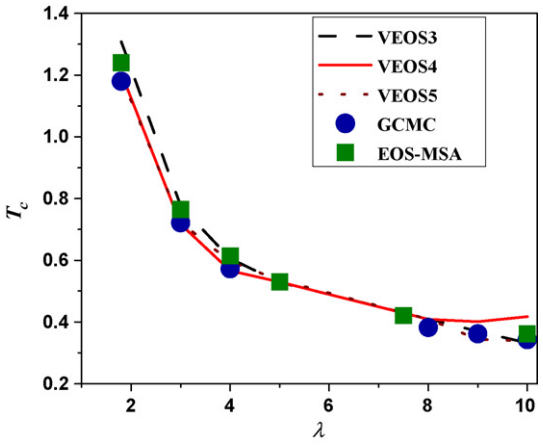

Fig. 10. Critical temperature, T_c^*, as a function of interaction range, λ. Lines represent the results of different truncated virial EOS. Filled circles represent the data of GC-TMMC [51]. Filled squares represent the data of EOS-MSA [47].

ful virial EOS to predict the PVT behavior along the saturated vapor line of hard-core Yukawa fluids.

Critical properties can easily be estimated from virial equation of state. The critical properties are determined from the following thermodynamic conditions [65]:

$$\left(\frac{\partial p}{\partial V}\right)_{T_c} = 0, \qquad \left(\frac{\partial^2 p}{\partial V^2}\right)_{T_c} = 0. \tag{18}$$

In order to solve the above equations, we have fitted our virial coefficient data to the following equation containing exponential based terms.

$$B_i(T) = f_0 + f_1 x + f_2 x^2 + f_3 x^3 + f_4 x^4 + \cdots\cdots \tag{19}$$

here, $x = \exp(1/T^*)$ and f_i are constants. The number of terms to be used in the above equation for a particular virial coefficient is dependent on the accuracy of the fit in representing the virial coefficient data.

We calculated critical properties; temperature T_c^*, density ρ_c^* and pressure P_c^* of Yukawa fluids at various interaction range parameters: λ = 1.8, 3.0, 4.0, 5.0, 8.0, 9.0, 10.0. These critical properties are estimated using the third (VEOS3), fourth (VEOS4) and fifth (VEOS5) order truncated virial EOS and compared with literature values. VEOS6 is not considered for critical property calculation due to inaccurate fit of the B_6^* data to an equation form. Table 8 presents all the estimated critical properties based on different truncated series. The literature values of estimated critical temperature of Yukawa fluids substantially varies as these properties are determined from different means such as perturbation theory [66], exact MSA [44], truncated MSA [47] up to fifth term, Gibbs ensemble Monte Carlo simulation (GEMC) [57,67] and grand-canonical transition matrix Monte Carlo simulation (GC-TMMC) [51]. The performance of different truncated VEOS for the estimation of critical temperature fluctuates with the interaction parameter. Fig. 10 presents the plot of critical temperature as a function of interaction range parameter, which clearly indicates that at lower interaction range parameter, λ = 1.8, 3.0 and 4.0), T_c^* determined from VEOS4 and VEOS5 are in good agreement with T_c^* predicted from GCMC simulation. On the other hand, T_c^* estimated using VEOS3 are in good agreement with that due to MSA approach. However, the variation from literature value is marginal. At higher λ values, 8.0, 9.0 and 10.0, critical temperature predicted by fifth order (VEOS5) truncated virial series are in good agreement with literature values compared to that based

Table 8
The critical temperature T_c^*, density ρ_c^* and pressure P_c^* of Yukawa fluids of variable interaction range, λ estimated from virial equation of state (VEOS) and compared with literature values.

λ	T_c^*	ρ_c^*	P_c^*	Source
1.8	1.307_1	0.362_2	0.150_7	This work (VEOS3)
	1.208_4	0.283_2	0.128_8	This work (VEOS4)
	1.192_2	0.268_2	0.117_2	This work (VEOS5)
	1.192_8	0.294_6		Smit and Frenkel[a]
	1.177_5	0.313_{13}		Lomba and Almarza[b]
	1.255	0.310	0.148	Henderson et al.[c]
	1.210	0.280		Caccamo et al.[d]
	1.24012	0.31864	0.14023	Der-Ming et al.[e]
	1.180_1	0.315_1	0.110_2	Singh[f]
	1.179	0.308	0.102	Gonzalez-Melchor et al.[g]
3.0	0.776_3	0.385_4	0.096_3	This work (VEOS3)
	0.718_1	0.275_3	0.068_2	This work (VEOS4)
	0.725_{16}	0.282_{21}	0.066_{19}	This work (VEOS5)
	0.715_{11}	0.375_{27}		Lomba and Almarza[b]
	0.764	0.37993	0.10529	Duh et al.[e]
	0.722_1	0.355_1	0.072_1	Singh[f]
	0.725	0.351	0.099	Gonzalez-Melchor et al.[g]
4.0	0.606_2	0.375_6	0.076_3	This work (VEOS3)
	0.565_3	0.266_4	0.055_3	This work (VEOS4)
	0.594_5	0.363_3	0.081_1	This work (VEOS5)
	0.576_6	0.377_{21}		Lomba and Almarza[b]
	0.61432	0.42805	0.099032	Der-Ming et al.[e]
	0.572_1	0.385_1	0.057_1	Singh[f]
	0.593	0.361	0.081	Gonzalez-Melchor et al.[g]
5.0	0.531_6	0.384_3	0.066_2	This work (VEOS3)
	0.529_{10}	0.386_5	0.067_1	This work (VEOS4)
	0.536_7	0.387_6	0.077_1	This work (VEOS5)
	0.541	0.472	0.112	Henderson et al.[i]
	0.53053	0.47292	0.099148	Der-Ming et al.[e]
8.0	0.413_9	0.411_8	0.054_2	This work (VEOS3)
	0.410_{11}	0.471_5	0.047_1	This work (VEOS4)
	0.410_9	0.250_4	0.055_2	This work (VEOS5)
	0.382_2	0.447_5	0.044_5	Singh[f]
9.0	0.370_1	0.352_2	0.044_2	This work (VEOS3)
	0.404_5	0.413_7	0.041_1	This work (VEOS4)
	0.344_1	0.250_6	0.031_2	This work (VEOS5)
	0.362_2	0.454_5	0.043_4	Singh[f]
	0.427	0.57		Hagen and Frenkel[h]
10.0	0.333_7	0.370_7	0.038_1	This work (VEOS3)
	0.416_4	0.560_4	0.036_1	This work (VEOS4)
	0.337_4	0.291_4	0.043_1	This work (VEOS5)
	0.362	0.653	0.121	Henderson et al.[i]
	0.36179	0.65284	0.12129	Der-Ming et al.[e]
	0.343_2	0.471_2	0.039_1	Singh[f]

[a] Reference [57].
[b] Reference [67].
[c] Reference [66].
[d] Reference [68].
[e] Reference [47].
[f] Reference [51].
[g] Reference [55].
[h] Reference [56].
[i] Reference [44].

on VEOS3 and VEOS4. Table 8 also presents the critical density and pressure obtained from VEOS along with literature data. It is apparent that VEOS5 is a suitable EOS for lower interaction range parameter, λ = 1.8 – 5.0 for the prediction of critical properties; on the other hand, at higher λ = 8.0, 9.0 and 10.0, VEOS3 compares favorably for the critical properties.

4. Conclusions

Virial coefficients up to sixth order are computed via Mayer sampling method for hard-core attractive Yukawa fluids. The calculated virial coefficients are used in virial EOS to predict the PVT behavior along the saturated vapor conditions and critical properties of Yukawa fluids. Along the saturated vapor phase of the coexistence curve, VEOS4 describes the PVT behavior extremely well at all values of λ. Addition of fifth and sixth virial coefficients affects insignificantly the VEOS series at a lower λ; on the other hand, at higher λ inclusion of B_5 and B_6 deteriorates the performance of VEOS along the saturation line. VEOS5 based prediction of critical properties is reasonable for lower interaction range parameter, λ = 1.8 – 5.0; conversely, at higher λ = 8.0, 9.0 and 10.0, addition of virial coefficient higher than B_3 do not improve the quality of VEOS and VEOS3 compares favorably for the critical properties. It is yet to be seen the effect of B_7 and higher order coefficients on the prediction of critical properties and the PVT behavior, which we plan to study in near future.

Acknowledgements

This work was supported by the Department of Science and Technology (grant no. SR/S3/CE10/2006) and Department of Atomic Energy, Govt. of India (grant no. 2006/20/36/05-BRNS).

References

[1] D.A. McQuarrie, Statistical Mechanics. University Science Books, 2000.
[2] J.O. Hirschfelder, C.F. Curtiss, R.B. Bird, Molecular Theory of Gases and Liquids, Wiley, New York, 1954.
[3] E.A. Mason, T.H. Spurling, The Virial Equation of State, vol. 2, Pergamon Press Ltd., London, 1969.
[4] A.J. Masters, J. Phys.: Condens. Matter 20 (2008) 283102.
[5] J. Merikanto, E. Zapadinsky, A. Lauri, I. Napari, H. Vehkamaki, J. Chem. Phys. 127 (2007) 104303.
[6] K.M. Benjamine, A.J. Schultz, D.A. Kofke, Ind. Eng. Chem. Res. 45 (2006) 5566–5573.
[7] A.V. Kalinichev, S.V. Churakov, Fluid Phase Equilib. 183–184 (2001) 271–278.
[8] K. Shida, K. Ohno, Y. Kawajoe, Y. Nakamura, J. Chem. Phys. 117 (2002) 9942–9946.
[9] M.P. Hodges, R.J. Wheatly, A.H. Harvey, J. Chem. Phys. 116 (2002) 1397–1405.
[10] M.P. Hodges, R.J. Wheatly, A.H. Harvey, J. Chem. Phys. 117 (2002) 7169–7179.
[11] L.G. MacDowell, C. Vega, J. Chem. Phys. 109 (1998) 5670–5680.
[12] E.M. Holleran, J. Chem. Thermodyn. 2 (1970) 779–786.
[13] K.O. Monago, Chem. Phys. 337 (2007) 125–134.
[14] D.J. Winzor, D.J. Scott, P.R. Wills, Anal. Biochem. 371 (2007) 21–25.
[15] L. Meng, Y.-Y. Duan, Fluid Phase Equlib. 258 (2007) 29–33.
[16] L. Meng, Y.-Y. Duan, L. Li, Fluid Phase Equlib. 226 (2004) 109–120.
[17] L. Meng, Y.Y. Duan, Fluid Phase Equilib. 238 (2005) 229–238.
[18] L. Meng, Y.Y. Duan, X.D. Wang, Fluid Phase Equilib. 260 (2007) 354–358.
[19] C. Tronopoulos, AIChE J. 20 (1974) 263–272.
[20] C. Tronopoulos, AIChE J. 21 (1975) 827–829.
[21] C. Menduina, C. McBride, C. Vega, Phys. Chem. Chem. Phys. 3 (2001) 1289–1296.
[22] C. Vega, C. McBride, C. Menduina, Phys. Chem. Chem. Phys. 4 (2002) 3000–3007.
[23] A.Y. Vlasov, X.-M. You, A.J. Masters, Mol. Phys. 100 (2002) 3313–3324.
[24] L.G. MacDowell, C. Menduina, C. Vega, E. de Miguel, Phys. Chem. Chem. Phys. 5 (2003) 2851–2857.
[25] L.G. MacDowell, C. Menduina, C. Vega, E. de Miguel, J. Chem. Phys. 119 (2003) 11367–11373.
[26] J.K. Singh, D.A. Kofke, Phys. Rev. Lett. 92 (2004) 220601.
[27] D.J. Naresh, J.K. Singh, Fluid Phase Equilib. 279 (2009) 47–55.
[28] K.M. Benjamin, J.K. Singh, A.J. Schultz, D.A. Kofke, J. Phys. Chem. B 111 (2007) 11463–11473.
[29] K.M. Benjamine, A.J. Schultz, D.A. Kofke, J. Phys. Chem. C 111 (2007) 16021–16027.
[30] H. Guerin, Physica A 304 (2002) 327–339.
[31] H. Guerin, Fluid Phase Equilib. 218 (2004) 47–56.
[32] S. Zhou, Colloids Surf. A: Physicochem. Eng. Aspects 262 (2005) 187–190.
[33] Y.-Z. Lin, Y.-G. Li, J.-D. Li, J. Mol. Liq. 125 (2006) 29–36.
[34] C. Caccamo, G. Pellicane, D. Costa, J. Phys.:Condens. Matter 12 (2000) A437–A442.
[35] F.W. Tavares, J.M. Prasusnitz, Colloid Polym. Sci. 282 (2004) 620–632.
[36] R. Tuinier, C. Gogelein, Eur. Phys. J. E. 27 (2008) 171.
[37] M. Gonzalez-Melchor, C. Tapia-Medina, L. Mier-y-Teran, J. Alejandre, Condens. Matter Phys. 7 (2004) 767–778.
[38] M.S. Murillo, High Energy Density Phys. 4 (2008) 49–57.
[39] P. Wette, I. Klassan, D. Holland-Moritz, T. Palberg, S.V. Roth, D.M. Herlach, Phys. Rev. E 79 (2009), 010501(R).
[40] M. Ginoza, J. Phys. F: Met. Phys. 17 (1987) L115–L118.
[41] J.S. Rowlinson, Physica A 156 (1989) 15–34.
[42] Y.-Z. Lin, Y.-G. Li, J.-F. Lu, W. Wu, J. Chem. Phys. 117 (2002) 10165–10172.
[43] H. Guerin, J. Mol. Liq. 139 (2008) 149–152.
[44] D. Henderson, L. Blum, J.P. Noworyta, J. Chem. Phys. 102 (1995) 4973–4975.

[45] Y. Tang, J. Chem. Phys. 118 (2003) 4140–4148.
[46] E. Waisman, Mol. Phys. 25 (1973) 45–48.
[47] D.-M. Duh, L. Mier-y-Teran, Mol. Phys. 90 (1997) 373–379.
[48] K.P. Shukla, J. Chem. Phys. 112 (2000) 10358–10367.
[49] Y.V. Kalyuzhnyi, P.T. Cummings, Mol. Phys. 87 (1996) 1459–1462.
[50] R. Tuinier, G.J. Fleer, J. Phys. Chem. B 110 (2006) 20540–20545.
[51] J.K. Singh, Molec. Sim., in press, doi:10.1080/08927020902787796.
[52] Y. Duda, A. Romero-Martinez, P. Orea, J. Chem. Phys. 126 (2007) 224510.
[53] C. Rey, L.J. Gallego, L.E. Gonzalez, D.J. Gonzalez, J. Chem. Phys. 97 (1992) 51215125.
[54] C. Hoheisel, R. Zhang, Phys. Rev. A 43 (1991) 5332–5336.
[55] M. Gonzalez-Melchor, A. Trokhymchuk, J. Alejandre, J. Chem. Phys. 115 (2001) 3862–3872.
[56] M.H.J. Hagen, D. Frenkel, J. Chem. Phys. 101 (1994) 4093–4097.
[57] B. Smit, D. Frenkel, Mol. Phys. 74 (1991) 35–39.
[58] D. Frenkel, B. Smit, Understanding Molecular Simulation: From Algorithms to Applications, 2nd ed., Academic Press, 2002.
[59] D.A. Kofke, Fluid Phase Equilib. 41 (2005) 228–229.
[60] D.A. Kofke, D. Frenkel, Handbook of Molecular Modeling, Springer, Netherlands, 2005, pp. 683–706.
[61] D.A. Kofke, B.C. Mihalick, Fluid Phase Equilib. 194 (2002) 327–335.
[62] N.F. Carnahan, K.E. Starling, J. Chem. Phys. 51 (1969) 635–636.
[63] D. Henderson, L. Mier-y-Teran, L. Blum, Fluid Phase Equilib. 130 (1997) 65.
[64] J.A. Barker, D. Henderson, J. Chem. Phys. 47 (1967) 2856–2861.
[65] S.I. Sandler, Chemical and Engineering Thermodynamics, 3rd ed., John Wiley & Sons, New York, 1999.
[66] D. Henderson, E. Waisman, J.L. Lebowitz, L. Blum, Mol. Phys. 35 (1978) 241–248.
[67] E. Lomba, N.G. Almarza, J. Chem. Phys. 100 (1994) 8367–8372.
[68] C. Caccamo, G. Giunta, G. Malescio, Mol. Phys. 84 (1995) 125–131.